

Daytime Geomagnetic Disturbances at High Latitudes during a Strong Magnetic Storm of June 21–23, 2015: The Storm Initial Phase

L. I. Gromova^a, N. G. Kleimenova^{b, c}, A. E. Levitin^a, S. V. Gromov^a,
L. A. Dremukhina^a, and N. R. Zelinskii^b

^a Pushkov Institute of Terrestrial Magnetism, Ionosphere, and Radiowave Propagation,
Russian Academy of Sciences, Troitsk, Moscow oblast, 142190 Russia

^b Schmidt Institute of Physics of the Earth, Russian Academy of Sciences,
Bol'shaya Gruzinskaya ul. 10, Moscow, 123995 Russia

^c Space Research Institute, Russian Academy of Sciences,
Profsoyuznaya ul. 84/32, Moscow, 117997 Russia

e-mail: gromova@izmiran.ru

Received December 28, 2015

Abstract—The high-latitude geomagnetic effects of an unusually long initial phase of the largest magnetic storm ($SymH \sim -220$ nT) in cycle 24 of the solar activity are considered. Three interplanetary shocks characterized by considerable solar wind density jumps (up to $50\text{--}60\text{ cm}^{-3}$) at a low solar wind velocity ($350\text{--}400$ km/s) approached the Earth's magnetosphere during the storm initial phase. The first two dynamic impacts did not result in the development of a magnetic storm, since the IMF B_z remained positive for a long time after these shocks, but they caused daytime polar substorms (magnetic bays) near the boundary between the closed and open magnetosphere. The magnetic field vector diagrams at high latitudes and the behaviour of high-latitude long-period geomagnetic pulsations (*ipcl* and *vlp*) made it possible to specify the dynamics of this boundary position. The spatiotemporal features of daytime polar substorms (the dayside polar electrojet, *PE*) caused by sudden changes in the solar wind dynamic pressure are discussed in detail, and the singularities of ionospheric convection in the polar cap are considered. It has been shown that the main phase of this two-stage storm started rapidly developing only when the third most intense shock approached the Earth against a background of large negative IMF B_z values (to -39 nT). It was concluded that the dynamics of convective vortices and the related restructuring of the field-aligned currents can result in spatiotemporal fluctuations in the closing ionospheric currents that are registered on the Earth's surface as bay-like magnetic disturbances.

DOI: 10.1134/S0016793216030051

1. INTRODUCTION

Different geomagnetic disturbances originate as a result of the solar wind effect on the Earth's magnetosphere. Global magnetic storms are among the most significant disturbances (e.g., (Akasofu and Chapman, 1972; Gonzales et al., 1994)). A magnetic storm is characterized by the formation of the ring current, as estimated by the *Dst* index, in the inner magnetosphere and the ionospheric currents (electrojets) in the auroral zone, which is characterized by the *AL* (westward electrojet) and *AU* (eastward electrojet) indices. A special class of polar magnetic disturbances is also distinguished (Troshichev and Tsyganenko, 1978; Troshichev et al., 1982). These disturbances are generated in the polar regions by different systems of field-aligned magnetospheric currents related to the effect of IMF and the solar wind on the magnetosphere.

The strongest magnetic storms are usually observed at the beginning of the solar cycle decline phase a year–a year and a half after the cycle maximum (e.g.,

(Zhang et al., 2007)). This is evidently illustrated by cycle 23 (Gonzalez et al., 2007). The present-day cycle 24 with an unusually low solar activity, the maximum of which was registered at the beginning of 2014, also confirms this circumstance. Two strong magnetic storms were observed during the decline phase of this cycle in 2015: on March 17–18 and June 21–23, 2015, when the *Dst* values reached $-(210\text{--}220)$ nT at the storm main phase maximum.

Much literature is devoted to the study of strong magnetic storms. The magnetic storm main phase, which develops against a background of southward IMF and high solar wind velocities, has been studied the most thoroughly. The largest geomagnetic disturbances are observed in the nightside sector during this storm phase. In this case intense auroral electrojets can move from auroral latitudes to midlatitudes and even to low latitudes. The magnetic storm initial phase, which is characterized by positive *Dst* values, has been studied least of all. Several researchers, e.g.,

(Loewe and Prolss, 1997), do not consider the existence of the magnetic storm initial phase, especially for storms with gradual commencement, and assume that this phase does not affect the development of the storm main phase. However, the physical processes in the Earth's magnetosphere are fundamentally different during the storm initial and main phases and develop in different magnetospheric domains.

During different storms, the storm initial phase duration varies from 10 min to several hours. This phase starts when an interplanetary shock reaches the Earth's magnetosphere and compresses it, causing an increase in the field strength in the magnetosphere and on the Earth's surface. Several researchers (e.g., (Schott et al., 1998; Kleimenova et al., 2000, 2011)) indicated that most intense geomagnetic variations and pulsations with periods of several minutes are observed in the dayside sector of polar latitudes during the storm initial phase.

The goal of the work is to analyze the initial phase of a great magnetic storm of June 21–23, 2015, and its daytime high-latitude geomagnetic effects in the Northern Hemisphere. This storm was caused by a double solar flare of M-class with the following three coronal mass ejections (www.izmiran.ru/services/) accompanied by three bursts of the solar wind dynamic pressure.

Note that the discussed magnetic storm occurred near the summer solstice, i.e., under the conditions of increased ionospheric conductivity of the north polar cap, when the solar plasma can directly penetrate the throat of the northern cusp. Consequently, most intense geomagnetic disturbances can be observed precisely in the north polar cap.

2. CONDITIONS IN THE SOLAR WIND AND IMF

Figure 1a shows the variations in the IMF B_y and B_z components, solar wind velocity (V) and density (Np), as well as the AL index of auroral magnetic activity and the $SymH$ index of the ring current intensity for June 21–23, 2015 (OMNI 1-min database, <http://nssdc.gsfc.nasa.gov/omniweb>). Note that the previous day (June 20) was very quiet ($Kp = 0$). According to the $SymH$ variations, the initial phase of the storm gradually started on June 21 as the appearance and slow increase in positive $SymH$ values after 12 UT. At that time, the solar wind density gradually increased at a constant very low solar wind velocity (~ 250 km/s), and the IMF B_y and B_z components fluctuated about zero.

At 1645 UT, the arrival of the first interplanetary shock was registered as an abrupt increase in the solar wind density from ~ 10 to ~ 50 cm^{-3} against a background of such quiet magnetic conditions. This arrival was accompanied by an insignificant increase in the velocity (from 270 to 350 km/s), as a result of which the solar wind dynamic pressure increased from 2 to 13 nPa.

According to classical views (Nishida, 1978), such an interplanetary shock structure can be interpreted as a fast shock arrival. The IMF B_y and B_z components abruptly increased to $\sim +5$ nT, and IMF B_y remained almost constant at about -10 nT and IMF B_z varied within ± 5 nT up to 22 UT. At about 22 UT, the IMF direction changed from southward into northward, and both components became positive. The solar wind velocity remained low (about ~ 350 km/s). Such conditions in the interplanetary medium did not allow a magnetic storm to develop in spite of a considerable solar wind impact.

The second shock with a similar structure approached the Earth's magnetosphere at 0644 UT on June 22, but the solar wind pressure jump was almost twice smaller, and the solar wind velocity abruptly increased from 350 to 420 km/s. In contrast to the first event, the IMF B_z values were negative at that time (to -10 nT) except a short positive impulse at about 06 UT, and the IMF B_y values were positive (to $+10$ nT).

The third, most intense, interplanetary shock approached the Earth's magnetosphere at 1838 UT on the same day. It can be considered an analog of SC , after which the storm main phase started developing very rapidly. However, the IMF B_z sign reversal from negative to positive at about 20 UT stopped the development of the storm main phase for a time, as was observed, e.g., during the main phase of a great magnetic storm that occurred on November 24, 2001 (Kleimenova et al., 2015).

3. DAYTIME HIGH-LATITUDE GEOMAGNETIC EFFECTS OF THE STORM INITIAL PHASE

Three very large jumps in the solar wind density were observed in the initial phase of the discussed storm: at 16.45 UT on June 21 and at 0544 and 1838 UT on June 22. We consider the high-latitude geomagnetic effects of these jumps. The data of observations on the IMAGE Scandinavian profile of stations and in the antipodal (North American) sector were used to analyze geomagnetic disturbances. The 1-min difference magnetograms of the geomagnetic field X and Y components were constructed for studies based on the method developed by A.E. Levitin (Levitin et al., 2013, 2014). Magnetic disturbances were calculated relative to the level of 2009 as the most magnetoquiet year. The use of difference magnetograms (Levitin et al., 2015; Kleimenova et al., 2015) makes it possible to eliminate quiet daily and secular variations.

Figure 1b shows the magnetograms of the individual stations on the IMAGE Scandinavian profile for June 21–23, 2015, the international codes and geomagnetic latitudes of which are presented on the plot right-hand axis. Most intense geomagnetic disturbances were observed during the storm main phase in

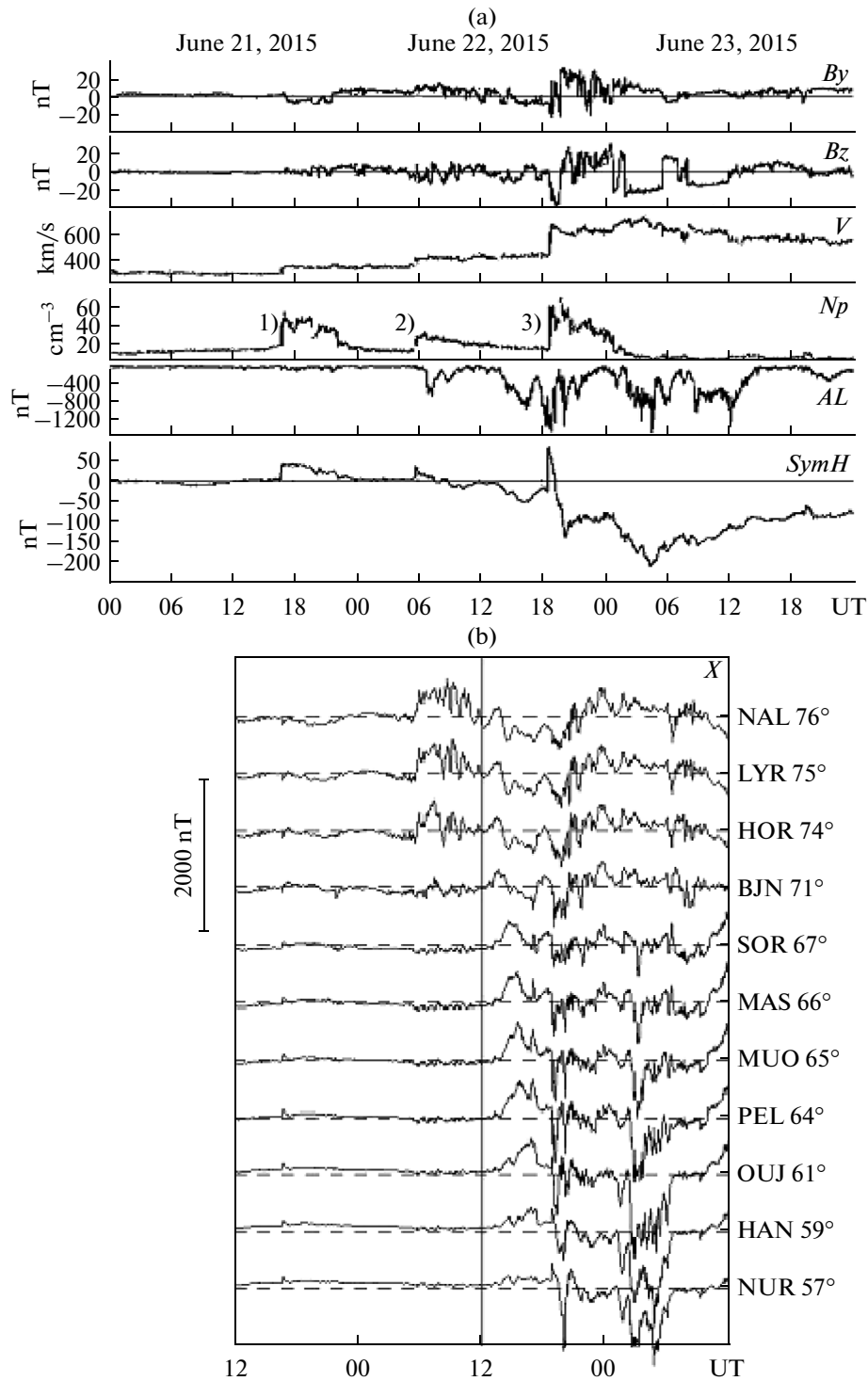


Fig. 1. (a) Variations in the solar wind and IMF parameters and the AL and $SymH$ geophysical indices on June 21–23, 2015; (b) magnetograms of the individual stations on the IMAGE Scandinavian profile.

the nightside sector as series of magnetospheric substorms at auroral and subauroral latitudes (MUO–NUR). During the storm initial phase, geomagnetic activity was most significant in the dayside sector of very high latitudes (HOR, LYR, NAL).

3.1. The First Shock (June 21, 1645 UT)

Before the arrival of the first shock to the Earth’s magnetosphere, the geomagnetic conditions in the near-Earth space was very quiet on June 20: the K_p index was equal to zero; AL was not larger than 50 nT;

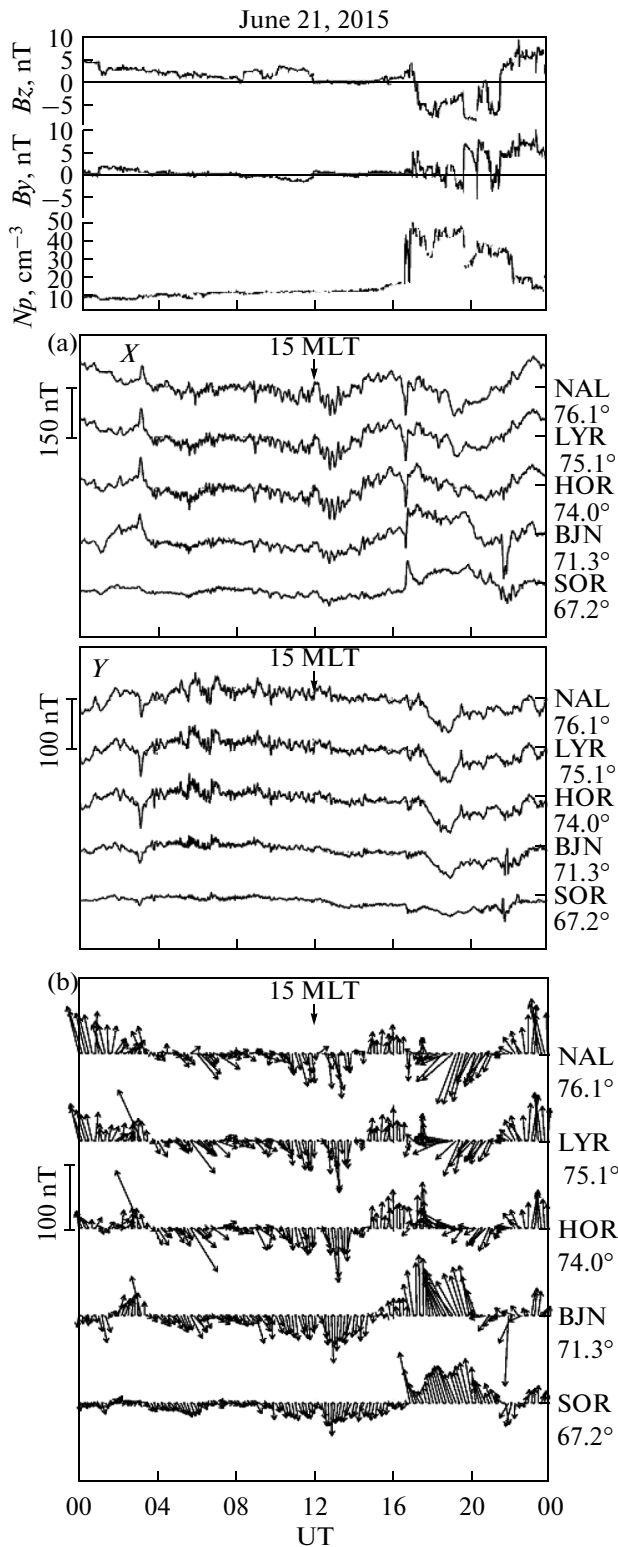


Fig. 2. Geomagnetic high-latitude effects of the arrival of the first, most intense, solar wind dynamic pressure jump on June 21, 2015: (a) magnetograms of the high-latitude observatories; (b) vector diagrams of magnetic disturbances.

$SymH$ fluctuated about zero up to 07 UT on June 21, was weak negative (to -10 nT) during the next five hours, and remained unchanged (at about $+10$ nT) from 12 UT to the shock arrival. The $SymH$ index suddenly increased to 50 nT as a result of the shock arrival. However, this sudden change did not result in the magnetic storm development, since the solar wind velocity remained low and the IMF B_z component was weak positive (Fig. 1a). Before the shock arrival, no considerable geomagnetic disturbances were registered on the Earth's surface; however, prolonged (lasting about seven hours at ~ 06 – 14 UT, i.e., at ~ 09 – 17 MLT) geomagnetic pulsations with periods of several minutes and an amplitude reaching ~ 40 nT (Fig. 2a), which is typical of the dayside polar cusp projection (*ipcl*, irregular pulsations cusp latitudes), were observed in the dayside sector at very high latitudes (NAL, LYR, HOR) (Bolshakova and Troitskaya, 1977; Troitskaya, 1985).

On the magnetograms of high-latitude observatories, the shock arrival (1645 UT, i.e., ~ 20 MLT at the IMAGE meridian) was observed as a sharp pulse in the magnetic field X component, which is negative at higher latitudes (NAL, LYR, HOR) and positive at lower latitudes (Fig. 2a). The pulse sign reversal was observed between BJN and SOR observatories. This makes it possible to assume that the projection of the boundary between open and closed field lines in the dusk sector was between BJN ($\Phi \sim 71^\circ$) and SOR ($\Phi \sim 67^\circ$). Unfortunately, the sea is located between these observatories; i.e., ground-based observations are absent. It is interesting to note the BJN pulse was initially negative and subsequently rapidly reversed its polarity and became positive as at lower-latitude observatories. This may result from the fact that the projection of this boundary rapidly moved toward BJN along latitude.

The magnetograms of the polar observatories in the near-noon (RES, CBB) and postnoon (THL, GDH) sectors are presented in Fig. 3a, which demonstrates the observatory geomagnetic coordinates and MLT. Figure 3a indicates that a negative magnetic bay started at polar latitudes in the prenoon (RES, CBB) and postnoon (THL, GDH) sectors, as well as in the dusk sector (NAL, LYR, HOR; Fig. 2a) when the IMF B_y sign reversed from positive to negative (the upper plots in Fig. 3a); i.e., the westward polar electrojet with the maximal amplitude in the prenoon sector at RES developed. Such disturbances in the polar region have long been known (e.g., (Nicol'skii, 1961; Feldstein, 1976)) and were called *the polar electrojet (PE)*. It was established (e.g., (Kuznetsov and Troshichev, 1977)) that these disturbances are maximal near the dayside polar cusp projection and are usually observed in summer when IMF $B_z > 0$. Researchers began to denote these disturbances as the *DP3* current system and polar disturbances controlled by the IMF B_y sign as *DPY* currents.

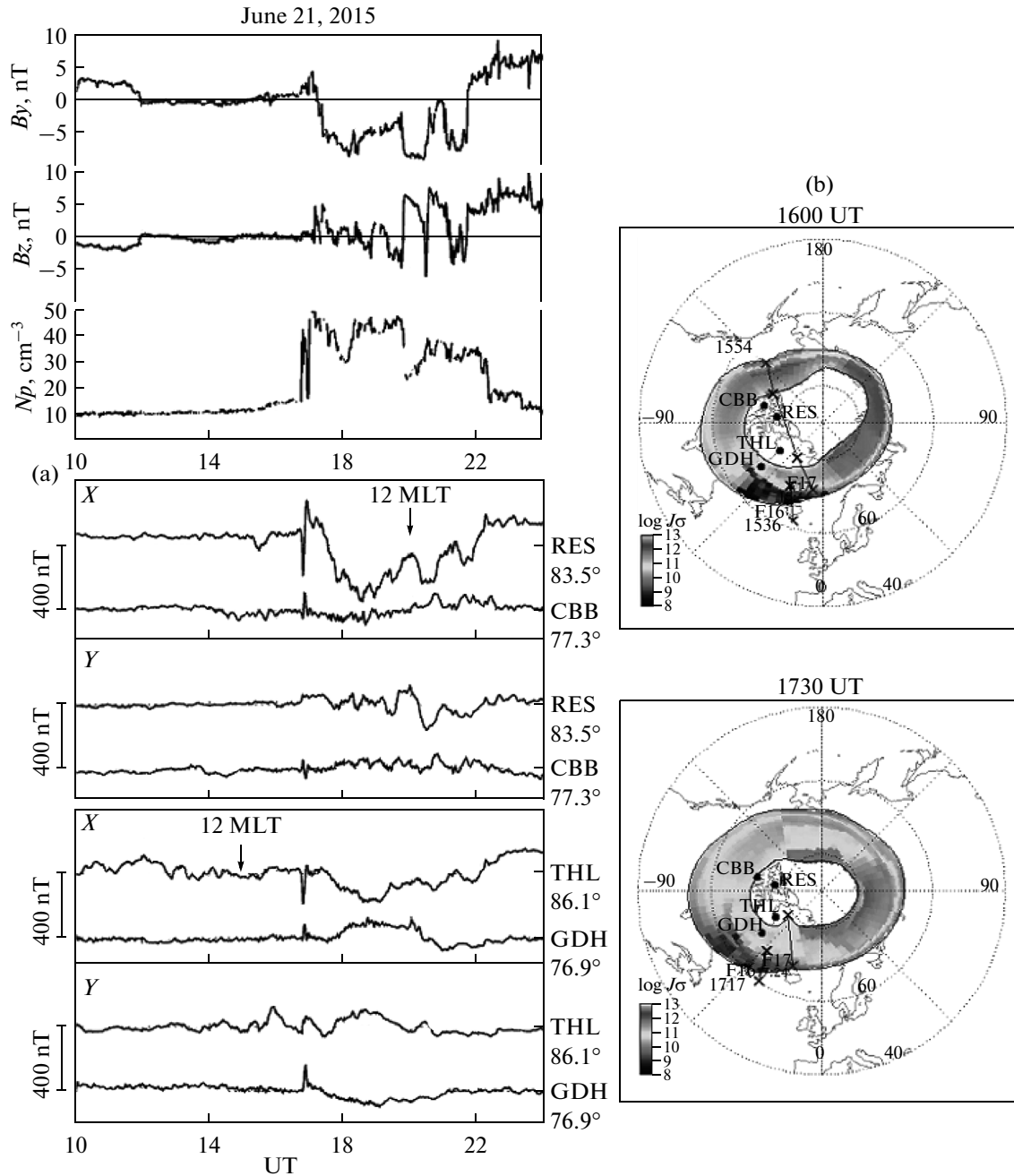


Fig. 3. (a) Difference magnetograms of the high-latitude observatories in the dayside sector during the first, most intense, solar wind dynamic pressure jump on June 21, 2015; (b) the auroral oval position according to the OVATION model.

The bay amplitude rapidly decreased with latitude and is almost imperceptible at CBB, which is located equatorward of RES by $\sim 6^\circ$. The bay sign is opposite in the postnoon sector at THL and GDH, which makes it possible to assume that the magnetospheric boundary was between these observatories as before the dynamic pressure jump arrival (different pulse polarity). This is also confirmed by the schematic location of the auroral oval presented in Fig. 3b, where the auroral oval position in the selected time interval according to the

OVATION model (http://sd-www.jhuapl.edu/Aurora/ovation/ovation_display.html) is shown in geographic coordinates. Figure 3b indicates that RES and THL were within the polar cap, CBB was near the cap boundary, and GDH was in the closed magnetosphere during the entire period under discussion.

In the dusk sector, the magnetic storm was first observed in the Y component and then in the X component of the magnetic field on the IMAGE Scandinavian profile (Fig. 2a). The vector diagram of high-

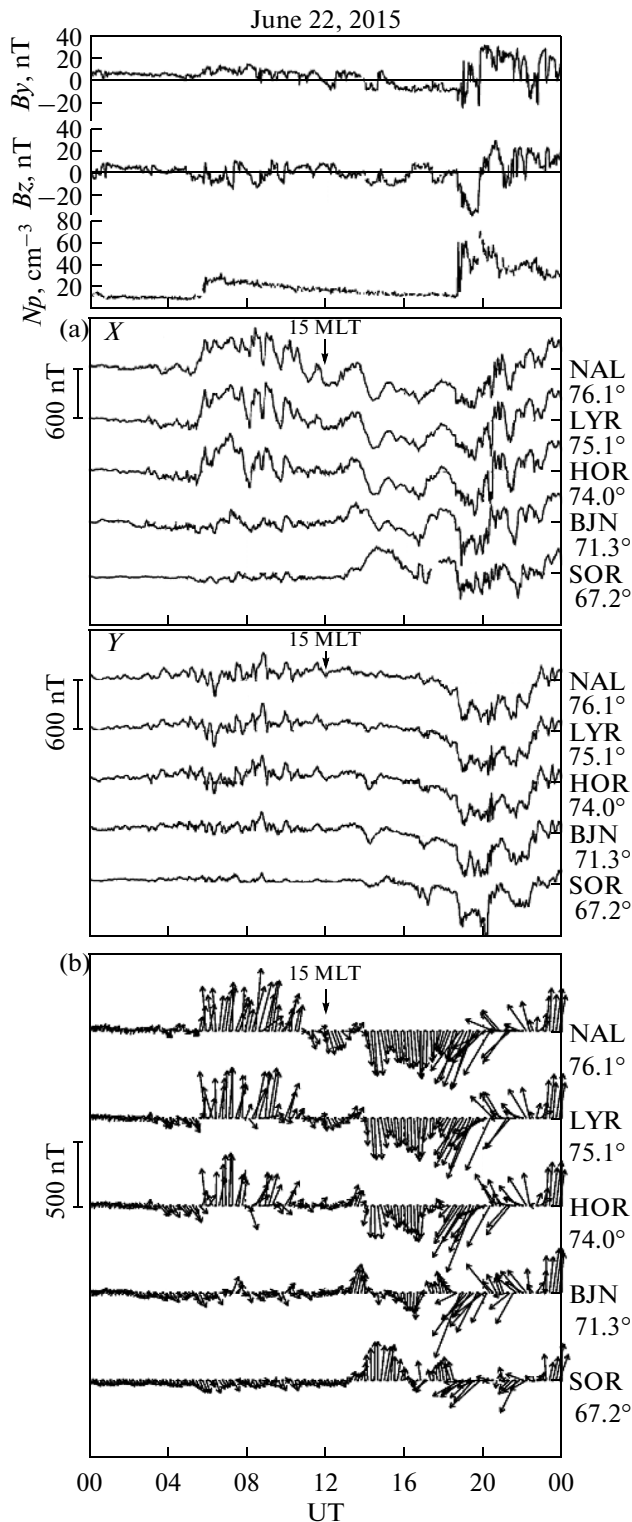


Fig. 4. The same as in Fig. 2, but for the second and third jumps of the solar wind dynamic pressure on June 22, 2015.

latitude geomagnetic variations presented in Fig. 2b indicates that the vortex sense of rotation at higher (NAL, LYR, HOR) and lower (BJN, SOR) latitudes was opposite. Note that vortex structures were not

observed in the magnetic field, and the field was directed identically at all latitudes before the arrival of the solar wind pressure jump to the Earth's magnetosphere. We can assume that all of these observatories were in the closed magnetosphere before the pressure jump, and only the lowest-latitude two observatories (BJN and SOR) remained in the closed magnetosphere after the jump, whereas the higher-latitude observatories (NAL, LYR, HOR) were in the region of the open field line projection.

3.2. The Second Shock (June 22, 0544 UT)

By the arrival of the second shock, the geomagnetic situation in the near-Earth space became quiet (Fig. 1a), and conditions similar to the period before the first shock arrival were formed. The solar wind dynamic pressure (density) jump was weaker in this case than in the first event but occurred against a background of negative IMF B_z values, which resulted in the development of auroral electrojets with AL values reaching ~ 600 – 700 nT. However, the storm main phase onset was hindered (Fig. 1a) by the appearance of positive IMF B_z values at ~ 09 – 14 UT.

The magnetograms at the high-latitude observatories on the IMAGE Scandinavian profile and the vector diagrams of high-latitude magnetic disturbances for June 22 are shown in Figs. 4a and 4b in the same format as was shown in Figs. 2a and 2b for June 21 but on a scale differing by a factor of 5, since more intense disturbances were observed at the end of that day. In addition, the arrival of the third, most intense, interplanetary shock at 1838 UT is shown in Figs. 4a and 4b.

The solar wind density jump at 0544 UT resulted in the generation of a daytime polar substorm (magnetic bay), which was registered before ~ 12 UT, i.e., from ~ 09 to ~ 15 MLT, at NAL, LYR, and HOR. A positive bay was observed in this case, which corresponds to eastward PE and is typical of IMF $B_y > 0$. Disturbances developed only in the field X component at that time, and the vectors were northward on the vector diagram (Fig. 4b) at NAL, LYR, and HOR; i.e., the ionospheric current flows along the parallel. A bay is absent at BJN. According to these data, we can assume that the projection of the boundary between closed and open geomagnetic field lines was located between HOR ($\Phi \sim 74^\circ$) and BJN ($\Phi \sim 71^\circ$).

At that time, a positive magnetic bay was observed in the antipodal (i.e., near-midnight) sector of polar latitudes (Fig. 5a, 22–02 MLT, RES, CBB) and in the dawn sector (04–09 MLT, THL, GDH). According to the OVATION model concepts, all of these observatories were located in the polar cap during the period under discussion (Fig. 5b).

3.3. The Third Shock (June 22, 1838 UT)

The arrival of the third shock was registered at the beginning of the storm main phase. A very consider-

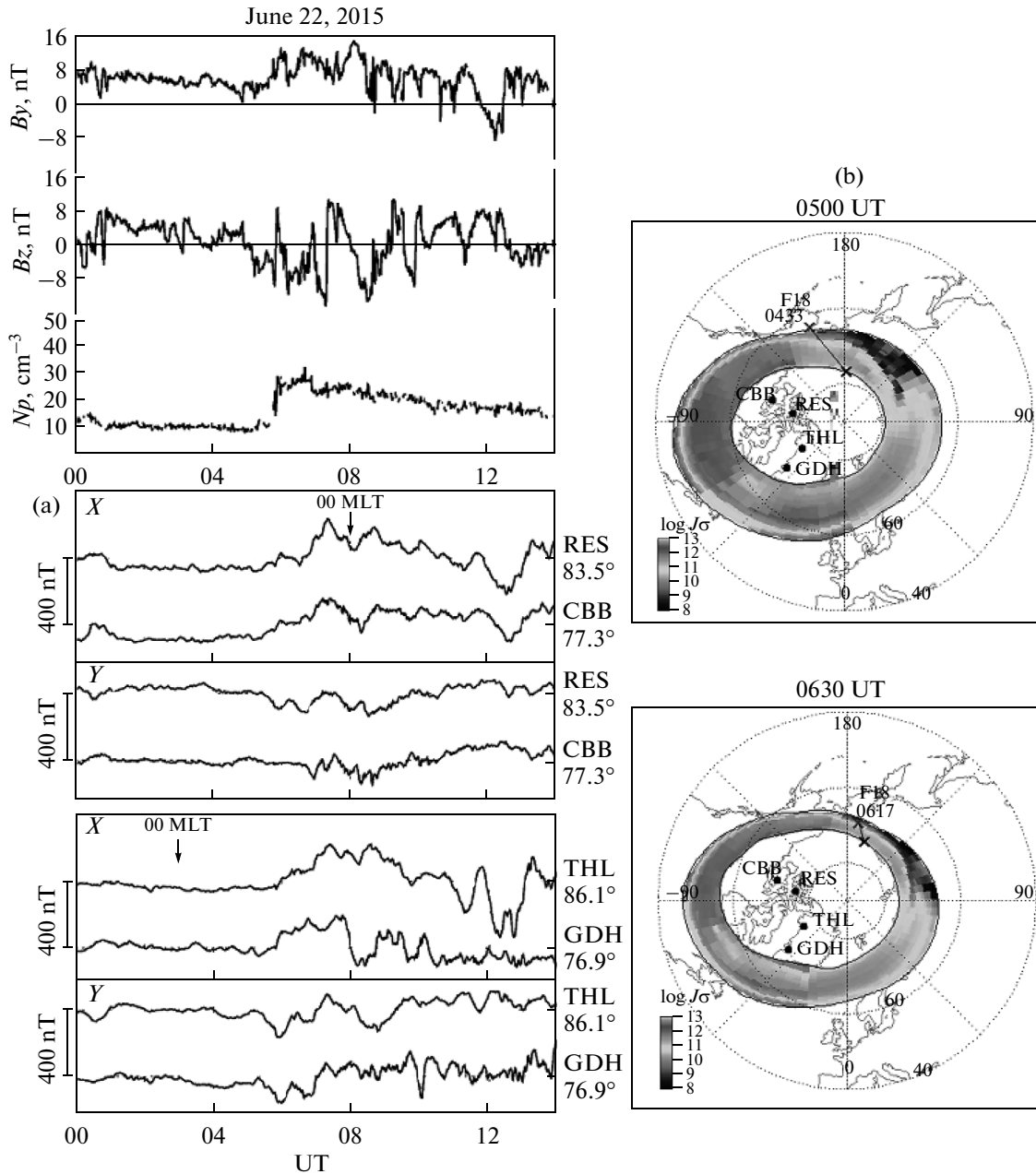


Fig. 5. The same as in Fig. 3, but for the second and third jumps of the solar wind dynamic pressure on June 22, 2015.

able (up to ~ 60 nPa) jump of the solar wind dynamic pressure, accompanied by a huge negative (about -40 nT) excursion in IMF B_z , caused an intense (about $+60$ nT) positive pulse in $SymH$ (Fig. 1a) and intense (up to ~ 1500 nT) electrojets at auroral latitudes. At that time, the Scandinavian meridian was in the dusk sector (21 MLT) of the magnetosphere; therefore, such a situation naturally resulted in the development of intense substorms. Note that two considerable intensifications were observed at ~ 61 – 67° geomagnetic latitudes (OUJ–MAS), which were combined into a very large intensification (Fig. 1b) at lower latitudes

(HAN–NUR). A magnetic bay of a slightly different configuration, accompanied by intense fluctuations, was also observed at polar latitudes, which is evident in Fig. 1b. This disturbance corresponded to the appearance of a left-handed vortex (Figs. 4a, 4b), which interrupted the previous negative magnetic disturbance caused by negative IMF B_y values.

3.4. Convection in the Polar Cap

It is known (e.g., (Moretto et al., 2000; Lukianova, 2004)) that the approach of the solar wind dynamic pres-

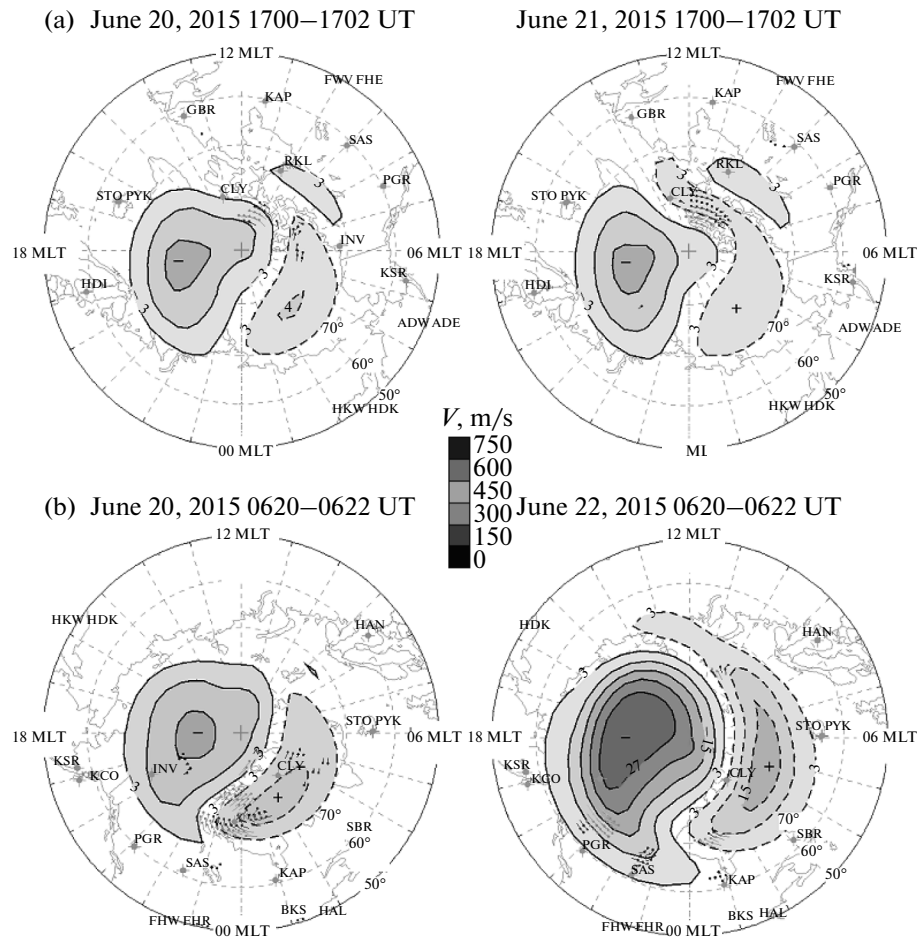


Fig. 6. Polar convection maps during (a) the first and (b) the second solar wind dynamic pressure jumps as compared to convection at the same UT instant on a very quiet day (June 20).

sure jumps to the Earth's magnetosphere affects the distribution of large-scale ionospheric plasma convection at high latitudes. The data of the SuperDARN ground radar system (<http://vt.superdarn.org/tiki-index.php?page=Conv+map+overview>), including the polar convection maps obtained by synthesizing the incoherent scatter radar observations and the known statistical models (e.g., (Cousins and Shepherd, 2010)), were used to consider variations in high-latitude convection caused by dynamic pressure (P_{sw}) jumps. Figure 6 presents the polar convection distribution during (a) the first and (b) the second solar wind dynamic pressure jumps. The convection patterns for the same UT intervals on the previous very quiet day (June 20), when all parameters of the solar wind plasma and magnetic field had minimal values and the IMF B_y and B_z remained close to zero for a long time (more than a day), are shown in Figs. 6a and 6b for comparison.

The first P_{sw} jump at 1645 UT on June 21 was caused by a sharp solar wind density jump without a considerable increase in the solar wind velocity. When the P_{sw} jump arrived, the IMF B_y component became negative and the IMF B_z component turned north-

ward. Figure 6a indicates that convection vortices were localized as before (within 70° geomagnetic latitude) after the P_{sw} front arrival. As compared to the quiet day (June 20), the morning vortex extended along longitude and reached the postnoon sector. In addition, polar convection vortices related to the formation of the system of the NBZ field-aligned currents, which were not observed on the quiet day (June 20), started forming. Such a convection pattern agrees with the conclusions made in (Lukianova, 2004). Note that a negative magnetic bay (Fig. 3a) was observed at that time on the Earth's surface near the pole from the morning (RES) to postnoon (THL) MLT hours at negative IMF B_y values; i.e., westward PE was observed.

As was indicated in (Belenkaya et al., 2004), the transient current system, which contains the NBZ field-aligned currents, the zone-1 currents, and the Pedersen ionospheric currents in the open field line region closing the currents indicated above, can develop in response to the compression of the magnetosphere under the action of the solar wind dynamic pressure jump at the positive IMF B_z component. The result of the appearance of such a transient current

system is that spreading currents are absent (during approximately 30–40 min) in the closed field line region and the magnetic field of the transient current system can be registered on the Earth since the Fukushima theorem is violated. A similar pattern was probably observed in the discussed case.

The polar convection distribution after the second P_{sw} jump on June 22 is presented in Fig. 6b, which shows the convection maps at 0620 UT on June 22 and at the same time on a very quiet day (June 20) for comparison. In contrast to the first P_{sw} jump (June 21), during the second P_{sw} jump, the IMF B_z and B_y values were negative and positive, respectively. It is clear that a considerable convection enhancement with the predominance of the evening vortex and the convection expansion toward lower latitudes (to 60° geomagnetic latitude) was observed after the arrival of the P_{sw} front as compared to the quiet day, which is also observed on the auroral oval location map at that time presented in Fig. 5b. In addition, the morning convection vortex considerably expanded along longitude toward the postnoon sector, and the potential drop through the polar cap increased by a factor of more than 1.5. A positive magnetic bay with a very wide longitudinal interval, extending from near-midnight (Fig. 5a, RES) to postnoon (Fig. 4a, LYR–NAL) MLT hours, was observed on the Earth's surface at that time, which indicates that extensive PE existed at IMF $B_y > 0$.

4. DISCUSSION

We noted above that special space weather conditions (Fig. 1a) resulted in an atypically long initial phase of one of the strongest magnetic storms in cycle 24 (observed on June 21–23, 2015), when the $SymH$ index values reached -220 nT during the storm main phase. Three interplanetary shocks characterized by enormous solar wind density jumps to $50\text{--}60\text{ cm}^{-3}$ approached the Earth's magnetosphere during the storm initial phase. Although these jumps were observed against a background of a relatively low ($\sim 350\text{--}400$ km/s) solar wind velocity, they caused considerable daytime geomagnetic disturbances at polar latitudes (PE).

The storm occurred near the summer solstice, i.e., under the conditions of increased ionospheric conductivity of the polar cap, when the solar plasma can directly penetrate into the northern cusp throat. This promoted the appearance of considerable magnetic disturbances in the north polar cap.

Figure 2a indicates that $ipcl$ geomagnetic pulsations typical of the dayside cusp latitudes (e.g., (Bolshakova and Troitskaya, 1977; Troitskaya, 1985; Kurazhkovskaya and Klain, 1997)) were observed in prenoon MLT hours at the highest-latitude observatories of the IMAGE profile (NAL, LYR, HOR) under very quiet geomagnetic conditions ($Kp = 0$) before the first shock arrival. Figure 7a shows these pulsations fil-

tered in the 2–7 mHz band typical of $ipcl$ oscillations. It is evident that most intense pulsations were observed at LYR and HOR. The pulsation amplitude considerably decreased with increasing and decreasing latitude. Such a latitudinal distribution of the pulsation amplitude indicates that these observatories were near the dayside cusp equatorial projection but in the closed magnetosphere at that time.

The arrival of the first dynamic pressure jump resulted in the compression of the magnetosphere, such that the Spitsbergen archipelago (NAL, LYR, HOR) was already outside the closed magnetosphere, i.e., within the polar cap by 1730 UT (Fig. 2b). Dayside PE with the maximal amplitude in the dayside sector (RES) appeared near the pole (Fig. 3a). At lower latitudes, $ipcl$ geomagnetic pulsations (Fig. 7b) typical of the cusp projection were registered at CBB. This makes it possible to assume that CBB was near the boundary between closed and open geomagnetic field lines, which is confirmed by the calculated (the OVATION model) position of the auroral oval (Fig. 3b). The convection map (Fig. 6a) indicates that convection was enhanced in the dawn sector of the polar region in this case.

The arrival of the second shock at 0544 UT caused the development of a daytime positive magnetic bay in a very wide longitudinal interval extending from noon to postnoon MLT hours (Figs. 3a, 5a). The convection maps (Fig. 6b) indicate that the morning convection vortex expanded into the postnoon sector. Intense field fluctuations, which can be considered among very long period (vlp) geomagnetic pulsations with periods about 15–40 min, e.g., in (Kleimenova et al., 1985, 1986; Bolshakova et al., 1987, 1988), were observed in the near-noon sector of polar latitudes (the IMAGE Scandinavian profile) against a background of this magnetic bay. These pulsations are observed only in summer (i.e., at a very high ionospheric conductivity) near the cusp polar boundary (i.e., outside the closed magnetosphere) with amplitudes reaching several hundreds of nanoteslas. In the Northern Hemisphere, vlp pulsations are as a rule registered when IMF B_y values are positive and IMF B_z values are negative, as was observed in the event under discussion. The appearance of vlp geomagnetic pulsations at NAL, LYR, and HOR indicates that these observation points were outside the closed magnetosphere. This is also observed on the auroral oval maps shown in Fig. 5b.

The generation of vlp pulsations can be related to instabilities near the dayside magnetopause in the region of reconnection in the low-latitude boundary layer (Bolshakova et al., 1987). Fluctuating field-aligned currents, the ionospheric effect of which on the Earth's surface will be registered as vlp geomagnetic pulsations (Bolshakova and Troitskaya, 1982; Kleimenova et al., 1986), can appear as a result of pul-

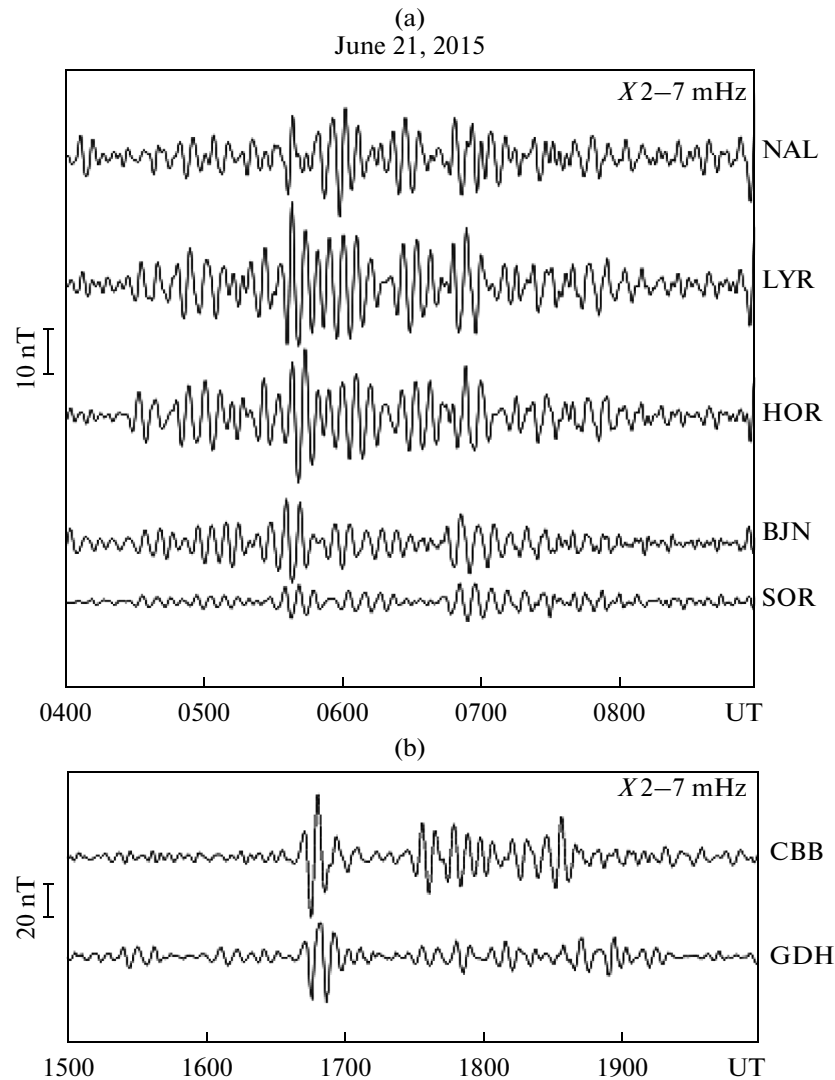


Fig. 7. *IpcI* geomagnetic pulsations on June 21, 2015, filtered in the 2–7 mHz band at (a) the high-latitude IMAGE stations at 04–09 UT and (b) CBB and GDH stations in the 15–20 UT interval.

sating transient reconnection at the magnetopause (flux transfer events, FTEs).

5. CONCLUSIONS

We studied the daytime high-latitude geomagnetic effects of an unusually long initial phase of the magnetic storm that occurred on June 21–23, 2015, which was among the largest ($SymH \sim -220$ nT) magnetic storms in cycle 24 of the solar activity. Three interplanetary shocks with considerable solar wind density jumps (up to $50\text{--}60\text{ cm}^{-3}$) at a low solar wind velocity (350–400 km/s) approached the Earth’s magnetosphere during this phase.

We indicated that the first two dynamic impacts did not result in the development of a magnetic storm, since the IMF B_z remained positive for a long time after these

impacts, but they caused daytime polar magnetic substorms (*PE*) in a wide interval of longitudes.

We concluded that the dynamics of convective vortices and the related reconfiguration of the field-aligned currents can result in spatiotemporal fluctuations in closing ionospheric currents, which can be registered on the Earth’s surface as intense magnetic bay-like disturbances (*PE*) at polar latitudes.

The constructed magnetic field variation vector diagrams at high latitudes and the behaviour of the observed high-latitude long-period geomagnetic pulsations (*ipcl* and *vlp*) made it possible to specify the spatiotemporal dynamics of the boundary between closed and open geomagnetic field lines.

We discussed in detail the spatiotemporal singularities of daytime polar substorms caused by solar wind dynamic pressure jumps and their relation to the IMF parameters. We indicated that only the third most

intense shock, which approached the Earth's magnetosphere against a background of very large negative IMF B_z values, resulted in the rapid development of the two-step main phase of this storm.

ACKNOWLEDGMENTS

The work performed by N.G. Kleimenova was supported by Presidium of the Russian Academy of Sciences (program 18); the work carried out by N.R. Zelinskii was supported by the Russian Foundation for Basic Research (project no. 16-35-00069 mol_a).

REFERENCES

- Akasofu, S.-I. and Chapman, S., *Solar–Terrestrial Physics*, Oxford: Clarendon, 1972; Moscow: Mir, 1975.
- Belenkaya, E.S., Alexeev, I.I., and Clauer, C.R., Field-aligned current distribution in the transition current system, *J. Geophys. Res.*, 2004, vol. 109, A11. doi 10.1029/2004JA010484
- Bol'shakova, O.V. and Troitskaya, V.A., Dayside cusp dynamics according to observations of long-period geomagnetic pulsations, *Geomagn. Aeron.*, 1977, vol. 17, no. 6, pp. 1076–1082.
- Bol'shakova, O.V. and Troitskaya, V.A., Pulse reconnection as a possible source of *ipcl*-type pulsations, *Geomagn. Aeron.*, 1982, vol. 22, no. 5, pp. 877–879.
- Bol'shakova, O.V., Klain, B.I., Kleimenova, N.G., and Kurazhkovskaya, N.A., Peculiarities of the latitudinal distribution of very long-period (*vlp*) geomagnetic pulsations, *Geomagn. Aeron.*, 1987, vol. 27, no. 1, pp. 109–114.
- Bol'shakova, O.V., Klain, B.I., Kleimenova, N.G., and Kurazhkovskaya, N.A., Polarization characteristics of high-latitude very long-period (*vlp*) geomagnetic pulsations, *Geomagn. Aeron.*, 1988, vol. 28, no. 5, pp. 836–838.
- Cousins, E.D.P. and Shepherd, S.G., A dynamical model of high-latitude convection derived from SuperDARN plasma drift measurements, *J. Geophys. Res.*, 2010, vol. 115, A12329. doi 10.1029/2010JA016017
- Feldstein, Y.I., Magnetic field variation in near pole region during magnetically quiet periods and interplanetary magnetic fields, *Space Sci. Rev.*, 1976, vol. 18, pp. 777–861.
- Feldstein, Y.I., Popov, V.A., Cumnock, J.A., Prigancova, A., Blomberg, L.G., Kozyra, J.U., Tsurutani, B.T., Gromova, L.I., and Levitin, A.E., Auroral electrojets and boundaries of plasma domains in the magnetosphere during magnetically disturbed intervals, *Ann. Geophysicae*, 2006, vol. 2, pp. 2243–2276.
- Gonzalez, W.D., Joselyn, J.A., Kamide, Y., Kroehl, H.W., Rostoker, G., Tsurutani, B.T., and Vasylunas, V.M., What is a geomagnetic storm?, *J. Geophys. Res.*, 1994, vol. 99, pp. 5771–5792.
- Gonzalez, W.D., Echer, E., Clua-Gonzalez, A.L., and Tsurutani, B.T., Interplanetary origin of intense geomagnetic storms ($Dst < -100$ nT) during solar cycle 23, *Geophys. Res. Lett.*, 2007, vol. 34, no. 6, L06101. doi 10.1029/2006GL028879
- Kleimenova, N.G., Bol'shakova, O.V., Troitskaya, V.A., and Friis-Cristensen, E., Two types of long-period geomagnetic pulsations near the equatorial boundary of the dayside polar cusp, *Geomagn. Aeron.*, 1985, vol. 25, no. 1, pp. 163–164.
- Kleimenova, N.G., Bol'shakova, O.V., Kurazhkovskaya, N.A., and Friis-Cristensen, E., Very long-period pulsations of the geomagnetic field in polar caps and their coupling with the ionospheric DPY-current, *Geomagn. Aeron.*, 1986, vol. 26, no. 6, pp. 985–989.
- Kleimenova, N.G., Kozyreva, O.V., Bitterly, M., and Schott, J.-J., Long-period (1–6 mHz) geomagnetic pulsations during the initial phase of the strong magnetic storm of February 21, 1994, *Geomagn. Aeron. (Engl. Transl.)*, 2000, vol. 40, no. 4, pp. 420–429.
- Kleimenova, N.G., Kozyreva, O.V., Manninen, J., Raita, T., Kornilova, T.A., and Kornilov, I.A., High-latitude geomagnetic disturbances during the initial phase of a recurrent magnetic storm (from February 27 to March 2, 2008), *Geomagn. Aeron. (Engl. Transl.)*, 2011, vol. 51, no. 6, pp. 730–740.
- Kleimenova, N.G., Gromova, L.I., Dremukhina, L.A., Levitin, A.E., Zelinsky, N.R., and Gromov, S.V., High-Latitude geomagnetic effects of the main phase of the geomagnetic storm of November 24, 2001 with the northern direction of IMF, *Geomagn. Aeron. (Engl. Transl.)*, 2015, vol. 55, no. 2, pp. 174–184.
- Kuznetsov, B.M. and Troshichev, O.A., On the nature of polar cap magnetic activity during undisturbed periods, *Planet. Space Sci.*, 1977, vol. 25, no. 1, pp. 15–21.
- Kuznetsov, S.N., Suvorova, A.V., and Dmitriev, A.V., Shape and size of the magnetopause associated with parameters of the interplanetary medium, *Geomagn. Aeron. (Engl. Transl.)*, 1998, vol. 38, no. 6, pp. 697–702.
- Levitin, A.E., Gromova, L.I., Gromov, S.V., and Dremukhina, L.A., How to recalculate the geomagnetic activity, in *Proc. of the 36th Annual Seminar "Physics of Auroral Phenomena"*, 2013, pp. 41–44.
- Levitin, A.E., Gromova, L.I., Gromov, S.V., and Dremukhina, L.A., Quantitative estimation of local geomagnetic activity relative to the level of the magnetically quiet period in 2009, *Geomagn. Aeron. (Engl. Transl.)*, 2014, vol. 54, no. 3, pp. 292–299.
- Levitin, A.E., Kleimenova, N.G., Gromova, L.I., Antonova, E.E., Dremukhina, L.A., Zelinsky, N.R., Gromov, S.V., and Malysheva, L.M., Geomagnetic disturbances and pulsations as a high-latitude response to considerable alternating IMF variations during the magnetic storm recovery phase (case study: May 30, 2003), *Geomagn. Aeron. (Engl. Transl.)*, 2015, vol. 55, no. 6, pp. 730–743.
- Loewe, C.A. and Prolss, G.W., Classification and mean behavior of magnetic storms, *J. Geophys. Res.*, 1997, vol. 102, no. A7, pp. 14209–14213.
- Lukianova, R.Yu., Effect of abrupt changes in the solar wind dynamic pressure on the polar cap convection, *Geomagn. Aeron. (Engl. Transl.)*, 2004, vol. 44, no. 6, pp. 691–702.
- Moretto, T., Ridley, A.J., and Engebretson, M.J., High-latitude ionospheric response to a sudden impulse event

- during northward IMF conditions, *J. Geophys. Res.*, 2000, vol. 105, pp. 2512–2530.
- Nikol'skii, A.P., Experimental proofs of the existence of the second zone of magnetic disturbances in the east Arctic, *Geomagn. Aeron.*, 1961, vol. 1, no. 6, pp. 959–964.
- Nishida, A., *Geomagnetic Diagnosis of the Magnetosphere* Berlin: Springer, 1978; Moscow: Mir, 1980.
- Schott, J.-J., Kleimenova, N.G., Bitterly, J., and Kozyreva, O.V., The strong *Pc5* magnetic pulsations in the initial phase of the great magnetic storm of March 24, 1991, *Earth, Planets Space*, 1998, vol. 50, pp. 101–106.
- Troitskaya, V.A., ULF wave investigations in the dayside cusp, *Adv. Space Res.*, 1985, vol. 5, no. 4, pp. 219–228.
- Troshichev, O.A. and Tsyganenko, N.A., Correlation between interplanetary geomagnetic field parameters and geomagnetic variations in polar caps, *Geomagn. Issled.*, 1978, no. 25, pp. 47–59.
- Troshichev, O.A., Gizler, V.A., and Shirochkov, A.V., Field-aligned currents and magnetic disturbances in the day-side polar region, *Planet. Space Sci.*, 1982, vol. 30, pp. 1033–1042.
- Zhang, J., Richardson, I.G., Webb, D.F., et al., Solar and interplanetary sources of major geomagnetic storms (*Dst* < 100 nT) during 1996–2005, *J. Geophys. Res.*, 2007, vol. 112, A10102. doi 10.1029/2007JA012321

Translated by Yu. Safronov